Modelling chronic toxicokinetics and toxicodynamics of copper in mussels considering ionoregulatory homeostasis and oxidative stress

Le, T.T.Y.; Nachev, M.; Grabner, D.; Garcia, M.R.; Balsa-Canto, E.; Hendriks, A.J.; ... ; Sures, B.

Environmental Pollution 287 (2021) 117645

Contents lists available at ScienceDirect

Environmental Pollution

journal homepage: www.elsevier.com/locate/envpol

Modelling chronic toxicokinetics and toxicodynamics of copper in mussels considering ionoregulatory homeostasis and oxidative stress☆

T.T. Yen Le [a,*], Milen Nachev [a], Daniel Grabner [a], Miriam R. Garcia [b], Eva Balsa-Canto [b], A. Jan Hendriks [c], Willie J.G.M. Peijnenburg [d,e], Bernd Sures [a]

[a] Department of Aquatic Ecology and Centre for Water and Environmental Research (ZWU), Faculty of Biology, University of Duisburg-Essen, D-45141, Essen, Germany
[b] Process Engineering Group, Spanish Council for Scientific Research, IIM-CSIC, 36208, Vigo, Spain
[c] Department of Environmental Science, Faculty of Science, Radboud University Nijmegen, 6525 HP, Nijmegen, the Netherlands
[d] Center for Safety of Substances and Products, National Institute for Public Health and the Environment, Bilthoven, 3720 BA, the Netherlands
[e] Institute for Environmental Sciences, Leiden University, 2311 EZ, Leiden, the Netherlands

ARTICLE INFO

Keywords:
Metals
Bivalve
Toxicokinetics
Toxicodynamics
ATPase enzyme
Oxidative stress

ABSTRACT

Chronic toxicity of copper (Cu) at sublethal levels is associated with ionoregulatory disturbance and oxidative stress. These factors were considered in a toxicokinetic-toxicodynamic model in the present study. The ionoregulatory disturbance was evaluated by the activity of the Na^+/K^+-ATPase enzyme (NKA), while oxidative stress was presented by lipid peroxidation (LPO) and glutathione-S-transferase (GST) activity. NKA activity was related to the binding of Cu^{2+} and Na^+ to NKA. LPO and GST activity were linked with the simulated concentration of unbound Cu. The model was calibrated using previously reported data and empirical data generated when zebra mussels were exposed to Cu. The model clearly demonstrated that Cu might inhibit NKA activity by reducing the number of functional pump sites and the limited Cu-bound NKA turnover rate. An ordinary differential equation was used to describe the relationship between the simulated concentration of unbound Cu and LPO/GST activity. Although this method could not explain the fluctuations in these biomarkers during the experiment, the measurements were within the confidence interval of estimations. Model simulation consistently shows non-significant differences in LPO and GST activity at two exposure levels, similar to the empirical observation.

1. Introduction

Toxicokinetic-toxicodynamic (TK-TD) models have been applied to simulate the time course of the processes that determine toxic effects. These models combine a simulation of the time course of uptake, biotransformation, and elimination of toxicants in the organism with a delineation of the time course of adverse effects and organism recovery (Ashauer et al., 2010). Due to their numerous advantages, these models have been increasingly applied and extended to the population level (Jager et al., 2011; Ashauer et al., 2013).

Copper (Cu) might cause adverse effects in organisms at concentrations exceeding the window of essentiality (Gomes et al., 2011). Among aquatic organisms, freshwater mussels are highly sensitive to acute Cu exposure (Wang et al., 2011; Giacomin et al., 2013), while bivalve mussels have been widely deployed in ecotoxicology studies (Caricato et al., 2019). Chronic exposure to Cu at sublethal concentrations might lead to both ionoregulatory disturbance and oxidative stress in freshwater bivalves (Jorge et al., 2013, 2018). The activity of the osmoregulatory enzymes Na^+/K^+-ATPase (NKA) has been investigated as a potential target of Cu effects (Jorge et al., 2013, 2018; Fan et al., 2016). Copper might inhibit NKA activity by binding covalently to thiol groups (Kone et al., 1990) or via specific interactions with the magnesium binding sites (Li et al., 1996), leading to ionoregulatory and osmotic disturbances (Grosell et al., 2002). The consideration of enzyme activities is further recommended based on the finding in the study of Cappello et al. (2015) that metabolomics should be included in evaluating the effects of pollutants on bivalve mussels.

Copper induces oxidative stress-related damages due to stimulated peroxidation of polyunsaturated fatty acids and subsequent formation of reactive oxygen species (Halliwell and Gutteridge, 1984; Nishikawa et al., 1997; Vijayavel et al., 2007; Gomes et al., 2011). Lipid peroxidation (LPO) is a major mode of toxic action by oxygen radicals (Rikans

☆ This paper has been recommended for acceptance by Maria Cristina Fossi.

* Corresponding author.
E-mail address: yen.le@uni-due.de (T.T.Y. Le).

https://doi.org/10.1016/j.envpol.2021.117645
Received 16 November 2020; Received in revised form 9 June 2021; Accepted 21 June 2021
Available online 26 June 2021

and Hornbrook, 1997) and increased LPO levels are usually followed by irreversible cell injury, an early signal of cell death (Poli et al., 1986; Maellaro et al., 1990; Reed, 1990). Antioxidant systems can modulate LPO and associated damages of cellular components. For example, glutathione S-transferase (GST) metabolises a number of reactive oxygen species. Therefore, LPO and GST activity have been used as biomarkers to assess the physiological status of organisms (Petala et al., 2009; Goswami et al., 2014; Coppola et al., 2019).

The present study aimed to develop a TK-TD model for simulating Cu accumulation and responses of the zebra mussel *Dreissena polymorpha* chronically exposed to waterborne Cu at sublethal levels, considering both ionoregulatory disturbance and oxidative stress. Although ATPases have been recommended as a useful biomarker in ecotoxicology (Kulac et al., 2013), NKA activity has been included in only a few studies (Bouskill et al., 2006). We attempted to develop a model that is applicable even with such limited measurements. The model was calibrated in the first step using published data that include measurements of NKA activity, and in the second step with experimental data from the present study. Considering the unique sensitivity of the stenohaline zebra mussel to the ionic composition of the external environment (Dietz et al., 1994), the experiment was carried out at various Na^+ concentrations in water.

2. Materials and methods

2.1. Model specification

In the model, chronic Cu toxicity is related to both ionoregulatory disturbance and oxidative stress (Fig. S1). Metal ions inhibit NKA activity by binding at the enzyme binding sites instead of forming a complex with ATP (Krstic et al. (2005). Transition metals, such as Cu, have more significant effects on NKA than on other enzymes (Krstic et al., 2005). In the present TK-TD model, the binding of Cu to NKA was related to the inhibition of NKA activity. In contrast, responses of antioxidant defence systems were linked to the concentration of internal unbound Cu.

2.2. Model characterisation

2.2.1. Toxicokinetics

The concentration of Cu accumulated ($C_{Cu,int}$; μg/g dw) is determined by the balance of uptake from water (the first factor), elimination, and growth dilution (the second factor).

$$\frac{dC_{Cu,int}}{dt} = k_{u,Cu} \times C_{Cu,w} - \left(k_{e,Cu} + g\right) \times C_{Cu,int} \quad (1)$$

The uptake from water is a function of the uptake rate constant k_u (L/g/d) and the dissolved Cu concentration in water $C_{Cu,w}$ (μg/L). Copper elimination from mussels is proportional to the elimination rate constant k_e (1/d). The growth dilution depends on the growth rate of mussels g (1/d).

2.2.2. Toxicodynamics

The TD section links Cu accumulation to the concentration of Cu at sites of toxic action and subsequently to biological responses.

2.2.2.1. Relationship between internal Cu concentration and Cu concentrations at active sites of toxic actions. The internal Cu concentration in soft tissues of mussels was assumed to be distributed into three fractions: Cu binding to free NKA (i.e. in Cu_NKA complexes [Cu_NKA]; μmol/g dw), Cu binding to Na-bound NKA (i.e. in Cu_Na_NKA complexes [Cu_Na_NKA]; μmol/g dw), and unbound Cu (i.e. not bound to NKA; [$Cu_{unbound}$]; μmol/g dw). In the presence of oxygen or other electron acceptors, Cu^+ is readily oxidised to Cu^{2+}, leading to a dominance of Cu^{2+} in biological systems (Arredondo and Nunez, 2005). Consequently, reactions of accumulated Cu that determine the complexes with NKA were specified for Cu^{2+}.

NKA activity was simulated based on the internal metal concentration, following Epstein and McIlwain (1966) suggestion that stimulation or inhibition of NKA activity was caused by internal ions, not by ions in the environment. In long-term exposure, NKA activity might recover from the metal-induced inhibition by increasing the number of enzyme molecules and/or increasing the turnover rate (Kulac et al., 2013). NKA_{new} represents this factor in the following reactions. As an inhibitor, Cu^{2+} can bind to both free (i.e., unbound) enzymes (NKA) and Na-bound enzymes (Na_NKA). In addition, enzyme kinetics are influenced by 1) the inactivation of enzymes due to binding to the inhibitor and 2) the synthesis of the enzyme, which is a function of the oxidation rate of the substrate:

where NKA_{new} (μmol/g dw) represents the amount of enzyme newly synthesised, as related to the oxidation of the substrate that releases the product (inorganic phosphate) P_1 (μmol/g dw); NKA_{nf} (μmol/g dw) represents the inactivated or non-functional enzyme related to the oxidation of the inhibitor that produces the inorganic phosphate P_2 (μmol/g dw); k_{a1} (g dw/μmol/d), k_{d1} (1/d), k_{a2} (g dw/μmol/d), k_{d2} (1/d), k_{a3} (g dw/μmol/d), and k_{d3} (1/d) are reaction (association and dissociation) rate constants; and M_{ATP1} and M_{ATP2} (1/d) are the rate constants characterising the inorganic phosphate production from the hydrolysis with the Na-bound enzyme and with the Cu-bound enzyme, respectively. In other words, they represent the turnover rate or molecular activity of ATP when NKA is bound with the activating ion Na^+ or with the inhibitor Cu^{2+}. The inclusion of NKA_{nf} reflects the influence of metal ions, such as Cu^{2+}, on the maximum NKA activity (Vasic et al., 1999; Krstic et al., 2005). Furthermore, NKA_{new} and NKA_{nf} were assumed to depend on the product of the oxidation of the substrate and the inhibitor (P_1 and P_2, respectively). The product of the oxidation, in turn, depends on the binding of NKA with Na^+ and Cu^{2+}. Therefore, the number of recovered and inactivated NKA could be expressed as a function of these binding equations:

$$NKA_{new} = k_{rec} \times [Na\_NKA] \quad (2)$$

$$NKA_{nf} = k_{inact} \times [Cu\_NKA] \quad (3)$$

where k_{rec} (/) and k_{inact} (/) are recovery and inactivation rate constants, representing the recovery of Na-bound NKA after the release of inorganic phosphate and the inactivation of Cu-bound NKA, respectively.

The density of the functional enzyme can be written based on the initial density (NKA_0) in combination with the amounts of newly synthesised and inactivated enzymes. These enzymes include free molecules and enzymes in complexes with the substrate and/or with the inhibitor:

$$NKA_t = NKA_0 - NKA_{nf} + NKA_{new} = [NKA] + [Na\_NKA] + [Cu\_NKA] + [Cu\_Na\_NKA] \quad (4)$$

In other words, the number of free pump sites can be described as follows:

$$[NKA] = NKA_0 - k_{inact} \times [Cu\_NKA] + k_{rec} \times [Na\_NKA] - [Na\_NKA] - [Cu\_NKA] - [Cu\_Na\_NKA] \quad (5)$$

The concentrations of complexes of NKA with activating Na^+ and inhibiting Cu^{2+} could be written as:

$$\frac{d[Na\_NKA]}{dt} = k_{a1} \times NKA \times ([Na_{int}] - [Na\_NKA] - [Cu\_Na\_NKA]) - (k_{d1} + M_{ATP1}) \times [Na\_NKA] \quad (6)$$

$$\frac{d[Cu\_NKA]}{dt} = k_{a2} \times NKA \times \left(\frac{C_{Cu,int}}{MW_{Cu}} - [Cu\_NKA] - [Cu\_Na\_NKA]\right) - (k_{d2} + M_{ATP2}) \times [Cu\_NKA] \quad (7)$$

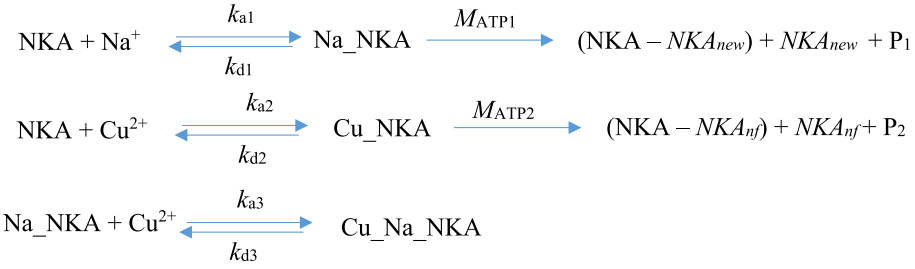

$$\frac{d[Cu\_Na\_NKA]}{dt} = k_{a3} \times [Na\_NKA] \times \left(\frac{C_{Cu,int}}{MW_{Cu}} - [Cu\_NKA] - [Cu\_Na\_NKA]\right) - k_{d3} \times [Cu\_Na\_NKA] \quad (8)$$

where $[Na\_NKA]$, $[Cu\_NKA]$, and $[Cu\_Na\_NKA]$ (μmol/g dw) are the concentrations of complexes of NKA with the activating Na^+ or/and the inhibitor Cu^{2+}; MW_{Cu} (g/mol) is the molecular weight of Cu; k_{a1} (g dw/μmol/d), k_{d1} (1/d), M_{ATP1} (1/d), k_{a2} (g dw/μmol/d), k_{d2} (1/d), M_{ATP2} (1/d), k_{a3} (g dw/μmol/d), and k_{d3} (1/d) are the rate constants explained above; and $[Na_{int}]$ (μmol/g dw) is the total internal Na concentration simulated by the method applied by Veltman et al. (2014), as such:

$$\frac{d[Na_{int}]}{dt} = \left(1 - \frac{NKA_{nf}}{NKA_0}\right) \times \frac{NKA_0 \times M_{Na}}{C_{Na,W} + K_{m,Na}} - \left(k_{e,Na} + g\right) \times [Na_{int}] \quad (9)$$

In the above equation, the deduction in the first factor represents the fraction of non-functional or inactivated NKA; M_{Na} (1/d) is the turnover rate determined by Veltman et al. (2014); $C_{Na,W}$ (mmol/L) is the concentration of Na^+ in water; $K_{m,Na}$ (mmol/L) is the apparent affinity of NKA for Na^+; and $k_{e,Na}$ (1/d) is the Na elimination rate.

2.2.2.2. Relationship between metal accumulation at active sites of toxic actions and toxic effects

2.2.2.2.1. Relation between the concentration of Cu-NKA complexes and inhibition of NKA activity. The model links the specific NKA activity to the rate at which inorganic phosphate is released, which is a function of the ATP hydrolysis with the activating ion Na^+ and the inhibitor Cu^{2+}:

$$v_S = \frac{1}{C_P} \times \frac{dP_1}{dt} = \frac{M_{ATP1} \times [Na\_NKA]}{C_P} \quad (10)$$

$$v_I = \frac{1}{C_P} \times \frac{dP_2}{dt} = \frac{M_{ATP2} \times [Cu\_NKA]}{C_P} \quad (11)$$

with C_P (mg protein/g dw) being the protein content.

With certain internal concentrations of Na and Cu, we could assume the change in the total amount of enzyme to be relatively small when the enzyme association and dissociation rates are much higher than the net rate at which the enzyme is lost or newly synthesised (See Mathematical elaboration of enzyme kinetics in the Supporting Information). Furthermore, decreases in NKA activity induced by inhibitors, such as Cu^{2+}, are related to the variations in the maximum velocities rather than the apparent affinity (K_m) (Vasic et al., 1999; Krstic et al., 2005). These results indicate non-competitive inhibition of NKA activity induced by Cu^{2+} (Krstic et al., 2005; Morgan et al., 1997). Therefore, the specific NKA activity can be derived according to the elaboration in the Supporting Information. Accordingly, the kinetics depend on the apparent affinity of NKA for Na^+ (K_m; μmol/g dw) and the inhibition constant of non-competitive inhibition between the activating ion and the inhibitor (K_I; μg/g dw):

$$K_m = \frac{k_{d1} + M_{ATP1}}{k_{a1}} \quad (12)$$

$$K_I = \frac{k_{d2} + M_{ATP2}}{k_{a2}} = \frac{k_{d3}}{k_{a3}} \quad (13)$$

The inhibition constant can be interpreted as the internal Cu concentration that inhibits NKA activity by 50%. The affinity of metals for thiol groups varies among metals, depending on their chemical properties and oxidative state (Buffle, 1988). McGeer et al. (2000) found that Ag^+ binds to NKA with a similar (i.e. within a factor of 2) binding constant as to the biotic ligand as determined by Paquin et al. (1999). Therefore, stability constants for binding of Na^+ and Cu^{2+} to biotic ligands (K_{NaBL} and K_{CuBL}; g/μmol) determined in the Biotic Ligand Model (BLM) were used to calculate their equilibrium dissociation constants:

$$\frac{1}{K_{NaBL}} = \frac{k_{d1}}{k_{a1}} \quad (14)$$

$$\frac{1}{K_{CuBL}} = \frac{k_{d2}}{k_{a2}} \quad (15)$$

The combination of the above equations with the apparent affinity generates the association and dissociation rate constants:

$$k_{d1} = \frac{M_{ATP1}}{K_m \times K_{NaBL} - 1} \quad (16)$$

$$k_{a1} = K_{NaBL} \times \frac{M_{ATP1}}{K_m \times K_{NaBL} - 1} \quad (17)$$

$$k_{d2} = \frac{M_{ATP2}}{K_I \times K_{CuBL} - 1} \quad (18)$$

$$k_{a2} = K_{CuBL} \times \frac{M_{ATP2}}{K_I \times K_{CuBL} - 1} \quad (19)$$

$$k_{d3} = k_{a3} \times k_I \quad (20)$$

2.2.2.2.2. Relationship between the concentration of internal unbound Cu and oxidative stress. A mechanistic understanding of the relationship between metal accumulation and oxidative stress is still limited. Therefore, LPO and GST activity were simulated by ordinary differential equations (ODEs) as applied in other TK-TD models:

$$\frac{dGST}{dt} = k_{acGST} \times ([Cu_{int}] - [Cu\_NKA] - [Cu\_Na\_NKA]) - k_{reGST} \times GST \quad (21)$$

$$\frac{dLPO}{dt} = k_{acLPO} \times ([Cu_{int}] - [Cu\_NKA] - [Cu\_Na\_NKA]) - k_{reLPO} \times LPO \quad (22)$$

where k_{acGST} and k_{acLPO} (units of GST or LPO/(μmol/g dw)/d) are the rate constants for damage accrual; and k_{reGST} and k_{reLPO} (1/d) regard the damage recovery rate constants.

The final model with eight state variables, i.e. total internal Cu concentration, total internal Na concentration, concentrations of complexes of NKA with Cu and/or Na, NKA activity, GST activity, and LPO, is given in SB, Supporting Information.

2.3. Model parameterisation

2.3.1. Initial functional NKA (NKA_0)

At high levels, salinity might influence the ouabain-binding that presents the functional binding sites of NKA (Piermarini and Evans, 2000; Lee et al., 2003). However, Sainting (1979) found no significant differences in the NKA density and molecular activity within a narrow range of salinity, up to 5 ppt. The initial number of functional NKA was parameterised assuming a negligible influence of salinity at low levels, as in our experiment or in the study of Jorge et al. (2013). Sainting (1979) investigated NKA activity and density in various tissues of bivalves, and showed the importance of considering NKA in other tissues (Table S2, Supporting Information). We applied the results by Sainting (1979), considering the relevance of NKA in various tissues. In particular, NKA_0 was derived from the NKA density in the mantle, gill, and foot measured by Sainting (1979) (Table S3, Supporting Information) and the total protein contents in these organs, as measured by Waykar and Lomte (2001). This approach yields a value of 2.17 pmol/mg protein for NKA_0^p. This value is in the density range of 2–100 pmol/mg protein reported in previous studies (Table S1, Supporting Information).

2.3.2. Molecular activity (M_{ATP1})

With low salinity levels in the experiment of the present study for the zebra mussel as well as in the study of Jorge et al. (2013), molecular activity or turnover rate of NKA was parameterised assuming a negligible influence of salinity based on the findings of Sainting (1979). Previous studies (Turner et al., 2005; Else et al., 1996) have reported a wide range of NKA molecular activity, from 1,5000 to 29,000 ATP/min, depending on organism size and tissues. The molecular activity reported for NKA in various tissues of marsh clam of *Rangia cuneata* by Sainting (1979) was comparable to the range found by Else et al. (1996) for ectothermic tissues. We used an average value derived from the molecular activity determined for the mantle, gill, and foot by Sainting (1979), i.e. $M_{ATP1} = 1737$ (1/min).

2.3.3. Apparent affinity for Na^+ for determining NKA activity and sodium uptake

Towle (1984) found a negligible correlation between the affinity of Na^+ for stimulating NKA activity (K_m) and the affinity for modelling Na^+ uptake, attributed to an absence of the enzyme at the controlling site for whole-animal Na^+ uptake. Therefore, the apparent affinity of NKA for Na^+ determined from the measurement of NKA activity was considered for simulating NKA kinetics (K_m) and the affinity determined from measurement of sodium uptake ($K_{m,Na}$) was used for modelling the internal Na concentration. In freshwater organisms, metal exposure (Morgan et al., 1997; Bury et al., 1999; Vasic et al., 2009) and salinity (Garcon et al., 2009) do not affect the affinity of NKA for Na^+. Accordingly, the affinity of NKA for Na^+ was parameterised using data in previous studies. We applied an average value of 9.74 (±7.83) mmol/L or µmol/g ww (Table S4, Supporting Information), which equals 173.26 µmol/g dw with a conversion factor of 0.056 (±0.003) between dry weight and wet weight determined from our measurements for the zebra mussel in the present study. A value of 0.205 mmol/L was derived for $K_{m,Na}$ from a compilation of previous studies (Table S5, Supporting Information).

2.3.4. Inhibition constant for Cu

Vasic et al. (1999) investigated the inhibition of NKA activity in synaptic plasma membrane isolated from rats by Cu. They found that NKA activity was inhibited by 50% at the concentration of 7.06 µmol/L or $7.06 \cdot 10^{-3}$ µmol/g.

The values for parameterised parameters are given in Table 1.

Table 1
Values of parameters parameterized for model calibration.

Parameter	Symbol	Value	Unit
Turnover rate of the NKA for releasing inorganic phosphate from the Na_NKA complexes	M_{ATP1}	2,501,280	1/d
Apparent affinity of NKA for Na	K_m	9.74 173.26	mmol/L µmol/g dw
Stability constant for binding of Cu^{2+} to NKA (in logarithm)	$\log K_{CuBL}$	8.02	L/mol
Stability constant for binding of Na^+ to NKA (in logarithm)	$\log K_{NaBL}$	2.91	L/mol
The initial density of functional pump sites	NKA_0	$1.45 \cdot 10^{-3}$	µmol/g dw
Inhibition rate constant induced by Cu on NKA activity	K_I	0.00706	umol/g
Total protein content	Cp	666.655	mg protein/g dw
Apparent affinity of NKA involved in sodium uptake for Na	K_{mNa}	0.205	mmol/L
Turnover rate of NKA for transporting Na^+	M_{Na}	$5.1 \cdot 10^5$	1/d
Molecular weight of Cu	MW_{Cu}	63.55	g/mol

2.4. Structural identifiability and sensitivity analyses

The model was checked for structural identifiability using GenSSI2 (Chis et al., 2011; Ligon et al., 2018). Results of structural identifiability analyses indicate the possibility of delivering a unique solution for the unknown parameters with noise-free data. The analysis showed that the model was structurally identifiable, with several parameters being globally identifiable.

A global sensitivity analysis was carried out using this toolbox to rank the unknown parameters regarding their influence on model estimation (Balsa-Canto et al., 2010). Results of the analysis unravelled the order: $M_{ATP2} > k_{reGST} > k_{e,Cu} > k_{u,Cu} > k_{e,Na} > k_{reLPO} > k_{a3} > k_{acLPO} > k_{acGST} > k_{inact} > k_{rec}$. In other words, model estimation was least sensitive to k_{rec}.

2.5. Model calibration

The model was calibrated using data from Jorge et al. (2013) using the MATLAB-based AMIGO toolbox as applied in our previous studies (Le et al., 2018, 2020). The parameters that describe NKA kinetics (k_{inact}, k_{rec}, M_{ATP2}, and k_{a3}) were considered for calibration and simulation in the next step. Considering the least sensitivity of the model estimation to the NKA recovery rate constant (k_{rec}), this parameter was removed in a subsequent calibration. In the calibration, the influence of growth dilution on Cu and Na accumulation was assumed to be negligible, considering the food unavailability during the experiment. The model was then calibrated using data for the zebra mussel generated from the experiment described in detail in Le et al. (2021) and in brief in the following section. The data used included: 1) the average of the daily dissolved Cu concentration (Table S6, Supporting Information) representing the Cu exposure level; 2) the concentration of Cu accumulated in the zebra mussel tissue presented in detail in Le et al. (2021) while raw data are given in Tables S7 (control), S8 (25 µg/L), and S9 (50 µg/L), Supporting Information; and 3) measurements of the biomarker responses (GST activity and LPO) achieved from the following experiment and presented in Figs. S2 and S3, Supporting Information, respectively.

2.6. Generation of data for model calibration

2.6.1. Exposure experiment

The exposure experiment was implemented in experimental fish facilities at the Department of Aquatic Ecology, Faculty of Biology, the University of Duisburg-Essen, which had been granted for the maintenance of animals for scientific purposes (Ordnungsamt Stadt Essen, Aktenzeichen: 32-2-11-80-71/199). The exposure experiment was

described in detail in Le et al. (2021). In brief, zebra mussels were collected from river Stever, North-Rhine Westphalia, Germany, between the Hullerner and the Halterner reservoirs (Le et al., 2020, 2021). In the laboratory, the mussels were kept in a tank filled with reconstituted water (Osterauer et al., 2010) for a two-week acclimation period. Individuals with a shell length in the range of 16–22 mm were used as this size group is the most abundant among the sampled population; and body size in such a narrow range was demonstrated not to influence metal bioaccumulation in the zebra mussel (Le et al., 2020). Twelve glass tanks were filled with 10 L of aerated reconstituted water each to form 4 exposure sets with different Na^+ concentrations. In addition, sodium was added as NaCl to the reconstituted water to obtain final nominal concentrations of 0.5, 1.5, 2.7, and 4.0 mmol/L (corresponding to salinity levels of 0.03, 0.09, 0.17, and 0.25 ppt). Each set included three tanks: one without Cu addition (control) and two with Cu added from the copper-ICP-Standard solution (Cu in 2% HNO_3, 1 g/L; Carl-Roth GmbH + Co KG, Karlsruhe) to obtain nominal Cu concentrations of 25 and 50 μg/L.

A group of 40 mussels was taken before the exposure experiment for initial measurements. Subsequently, mussels were distributed randomly to the tanks, 360 mussels each (Le et al., 2020, 2021), for a 24-day exposure experiment. Water was renewed daily. Water samples were taken before and after water exchange with filtration through a cellulose nitrate filter (pore size 0.45 μm, Sartorius AG, Goettingen, Germany) to determine dissolved metal concentrations. The experiment was carefully performed to minimise the stress to animals. Mussels were observed daily before and after water renewal for their shell opening. Forty mussels were randomly sampled once every four days, among them 12 for measurements of Cu concentrations in the mussels, 8 for measurements of biomarkers, and the remaining for subcellular fractionation in another research. As described in Le et al. (2021), no mortality was observed in all sodium groups, and the formation of holes on the shells of mussels at low pH was not seen in these treatments. The similarity in the condition index between control mussels and Cu-exposed mussels, as well as between mussels sampled prior and during the experiment indicates negligible effects of the exposure on the energy status of mussels (see Le et al., 2021 for details). All mussels were frozen in liquid nitrogen and stored at −80 °C for further measurements.

2.6.2. Measurements of biomarkers

2.6.2.1. Mussel preparation. Soft tissues were quickly removed from the frozen mussels, and homogenised in TRIS buffer containing 10 mM sodium phosphate buffer saline at pH 7.4 at a ratio of 1: 10 w/v using an UltraTurrax tissue homogeniser. The homogenates were then centrifuged at 14,000×*g* and 4 °C for 15 min. Three aliquots of the supernatant were used for measurements of the biomarkers. Eight replicates were carried out for each sample.

2.6.2.2. Glutathione-S-transferase activity. The measurement of GST activity was performed according to Habig et al. (1974), by spectrophotometrically measuring the increase in absorbance of the acceptor substrate 1-chloro-2,4-dinitrobenzene (CDNB, Sigma Aldrich) with reduced glutathione over time using the Infinite microplate reader (Tecan Infinite 200 PRO). A final volume of 200 μL contained 10 mM phosphate buffer pH 6.5, 1 mM CDNB, 1 mM glutathione, and 5 μL of the sample. GST activity was measured at 340 nM using a molar extinction coefficient of 9.6 mM^{-1} cm^{-1}.

2.6.2.3. Lipid peroxidation. Lipid peroxidation was assessed from the formation of 2-thiobarbituric acid reactive substances (TBARS) (Buege and Aust, 1978). In principle, peroxide products, such as TBARS, were determined by reference to the absorbance of malonedialdehyde (MDA) standards at 532 nm (Ohkawa et al., 1979). Sub-samples (110 μL) of tissue homogenate were treated with 27.5 μL of 8.1% sodium dodecyl sulfate and 440 μL of the staining agent (containing 10% trichloric acid pH 3.5 and 0.5% thiobarbituric acid). The mixture was boiled in a water bath at 95 °C for 20 min. After cooling, the mixture was shaken vigorously and centrifuged at 4000×*g* and 4 °C for 10 min. The fluorescence of obtained supernatant was measured at 532 nm. The concentration of TBARS was calculated from an external standard curve of 1,1,3,3-tetramethoxy propane (a stabilised form of MDA) (Barata et al., 2005). The total protein concentration was spectrophotometrically quantified according to Lowry et al. (1951) with Bovine Serum Albumin as a standard using the Infinite ® 200 PRO microplate reader (Tecan).

3. Results

3.1. Model calibration for Lampsilis siliquoidea

Calibration results displayed a steady inactivation of Cu-bound NKA as shown by gradual increases in the number of non-functional NKA, approaching the number of functional NKA (Fig. S4, Supporting Information). A steady increase in the number of non-functional NKA and a negligible recovery of NKA contributed to a gradual decrease in the number of functional NKA (Fig. S4, Supporting Information). Together with a largely inhibited turnover rate of Cu-bound NKA (Table 2), this contributes to an inhibition of NKA activity (Fig. 1). An instant and rapid decline in NKA activity and the internal Na concentration was observed within the first days of exposure as predicted by the model as well,

Table 2
Values of parameters calibrated for freshwater mussels *Lampsilis siliquoidea* (Jorge et al., 2013).

Parameter	Symbol	Value		Unit
		Full version	Reduced version	
Na^+ elimination rate constant	$k_{e,Na}$	17.90 (±130)	17.89 (±50.74)	1/d
Recovery rate constant representing the recovery of NKA from the release of inorganic phosphate from the Na_NKA binding	k_{rec}	0.0002 (±4186)	0	/
Cu uptake rate constant	$k_{u,Cu}$	0.39 (±0.20)	0.39 (±0.20)	L/g/d
Cu elimination rate constant	$k_{e,Cu}$	0.01 (±0.03)	0.01 (±0.03)	1/d
Inactivation rate constant representing the inactivation of NKA caused by the binding to Cu	k_{inact}	1 (±19)	1 (±7.28)	/
The turnover rate of Cu-bound NKA	M_{ATP2}	0.007 (±0.16)	0.007 (±0.05)	1/d
The association rate constant for binding of Cu to Na-bound NKA	k_{a3}	$1.64 \cdot 10^4$ ($\pm 5.18 \cdot 10^8$)	$1.64 \cdot 10^4$ ($\pm 3.10 \cdot 10^7$)	g dw/μmol/d
The damage accrual rate constant for the GST activity	k_{acGST}	4.85 (±14.67)	4.85 (±14.68)	μmol DNCB/min/mg protein/(μmol Cu/g dw)/d
The damage recovery for the GST activity	k_{reGST}	$1.72 \cdot 10^{-8}$ (±0.06)	$6.06 \cdot 10^{-8}$ (±0.06)	1/d
The damage accrual rate constant for LPO	k_{acLPO}	0.38 (±3.29)	0.38 (±3.28)	nmol TBARS/mg protein/(μmol Cu/g dw)/d
The damage recovery for LPO	k_{reLPO}	$1.90 \cdot 10^{-6}$ (±0.09)	$2.80 \cdot 10^{-5}$ (±0.09)	1/d

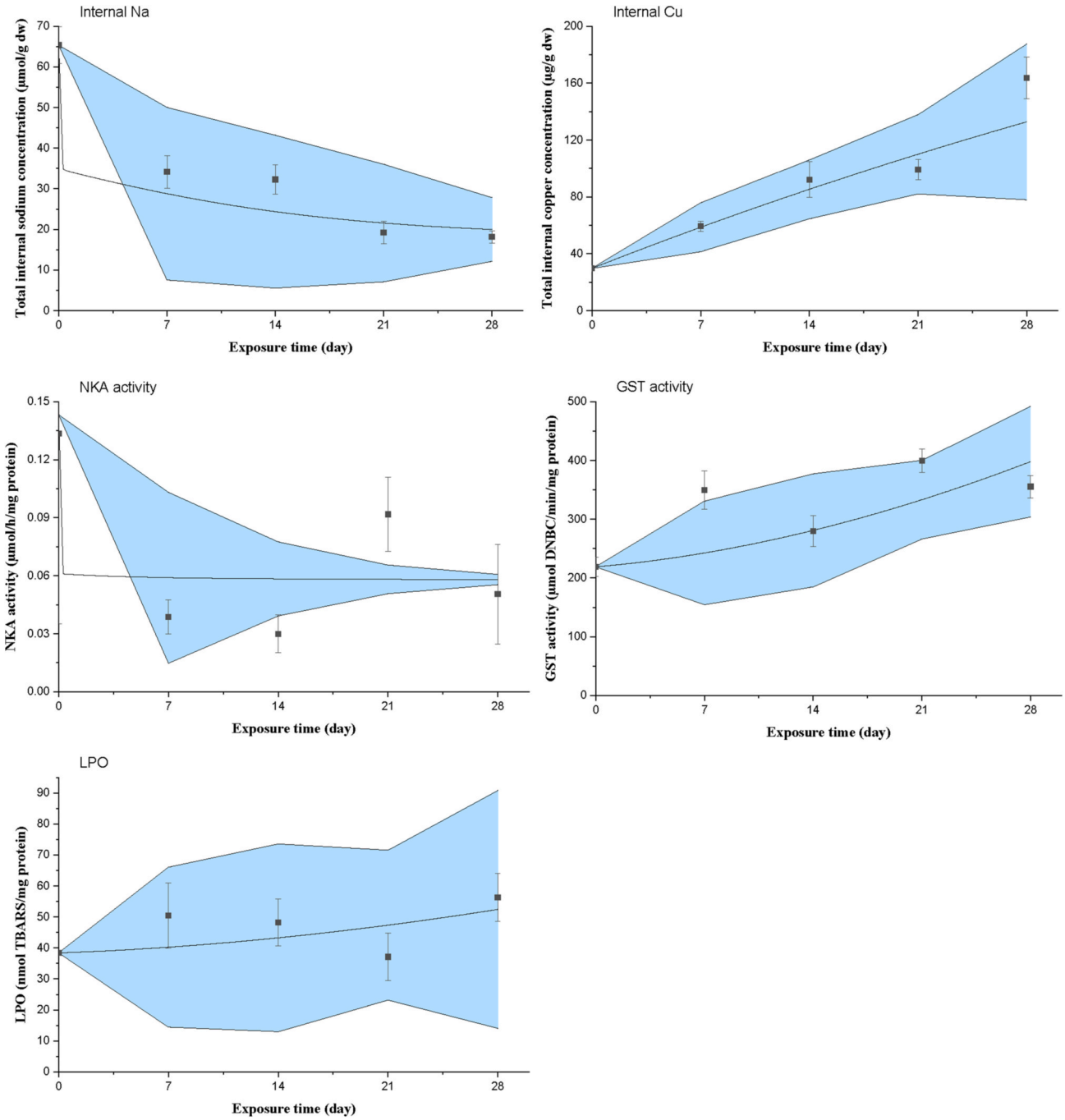

Fig. 1. Comparison between the modelled values and the measurements for total internal sodium concentration, total internal copper concentration, NKA activity, glutathione-S-transferase (GST) activity, and lipid peroxidation (LPO) in freshwater mussel *Lampsilis siliquoidea* exposed to Cu at a nominal concentration of 15 µg/L for 28 days. The areas and the solid lines in the middle of the areas represent the confidence internval and the mean of the estimations, respectively. The dots and bars represent the measurements (average and standard deviations, respectively).

followed by negligible decreases afterwards. GST activity was more sensitive to Cu exposure at a nominal concentration of 15 µg/L than LPO (Table 2; Fig. 1).

In general, the measurements for all factors (i.e. total Na concentration, total Cu concentration, GST activity, and LPO) were within the confidence interval of the estimations (Fig. 1) and within a factor of two of the estimation (Fig. S5, Supporting Information). However, the fluctuations in GST activity and LPO level could not be explained well by the model, which consistently generated an upward trend (Fig. 1). The limited sensitivity of the model estimation to the rate of NKA recovery (k_{rec}) unravelled by the global ranking analysis was further confirmed by little differences in calibration results with and without this parameter (Table 3). Such model reduction increased confidence, as shown by reduced confidence intervals of estimates (Table 3).

3.2. Model calibration for Dreissena polymorpha

The model simulation showed significant differences in the total internal Cu concentration between the two exposure levels, exhibited by non-overlapping confidence intervals (Fig. 2; Fig. S6, Supporting Information). Significant differences in the Cu uptake rate between the two exposure levels were found at Na^+ concentrations of 2.7 and 4.0

Table 3
Parameters describing toxicokinetics and toxicodynamics of copper in the zebra mussel calibrated at various exposure levels and Na concentrations in water.

Parameter	0.5 mmol/L Na		1.5 mmol/L Na		2.7 mmol/L Na		4.0 mmol/L Na	
	25 μg/L Cu	50 μg/L Cu	25 μg/L Cu	50 μg/L Cu	25 μg/L Cu	50 μg/L Cu	25 μg/L Cu	50 μg/L Cu
$k_{u,Cu}$	0.09 (±0.03)	0.08 (±0.008)	0.08 (±0.03)	0.11 (±0.03)	0.12 (±0.02)	0.09 (±0.005)	0.09 (±0.01)	0.14 (±0.02)
$k_{e,Cu}$	$4.13 \cdot 10^{-11}$ (±0.03)	$2.23 \cdot 10^{-16}$ (±0.01)	$3.67 \cdot 10^{-17}$ (±0.03)	0.005 (±0.025)	$5.55 \cdot 10^{-17}$ (±0.01)	$4.92 \cdot 10^{-16}$ (±0.01)	0 (±0.01)	0.03 (±0.02)
k_{acGST}	9.67 (±58)	5.43 (±26)	10 (±59)	6.72 (±35)	10 (±24)	9.41 (±41)	10 (±75)	9.21 (±74.45)
k_{reGST}	$1.22 \cdot 10^{-10}$ (±0.24)	$1.90 \cdot 10^{-15}$ (±0.18)	$1.51 \cdot 10^{-16}$ (±0.23)	$7.19 \cdot 10^{-14}$ (±0.25)	0.03 (±0.15)	0 (±0.23)	$4.33 \cdot 10^{-16}$ (±0.32)	$2.48 \cdot 10^{-12}$ (±0.48)
k_{acLPO}	5.12 (±21)	1.53 (±7.80)	1.78 (±7.69)	10 (±54)	10 (±30)	7.15 (±174)	1.37 (±8.02)	0.05 (±1.34)
k_{reLPO}	0.16 (±1.02)	$2.86 \cdot 10^{-13}$ (±0.61)	$4.24 \cdot 10^{-14}$ (±0.50)	0.63 (±3.94)	0.35 (±1.24)	1 (±26)	0 (±0.59)	$5.30 \cdot 10^{-12}$ (±0.62)

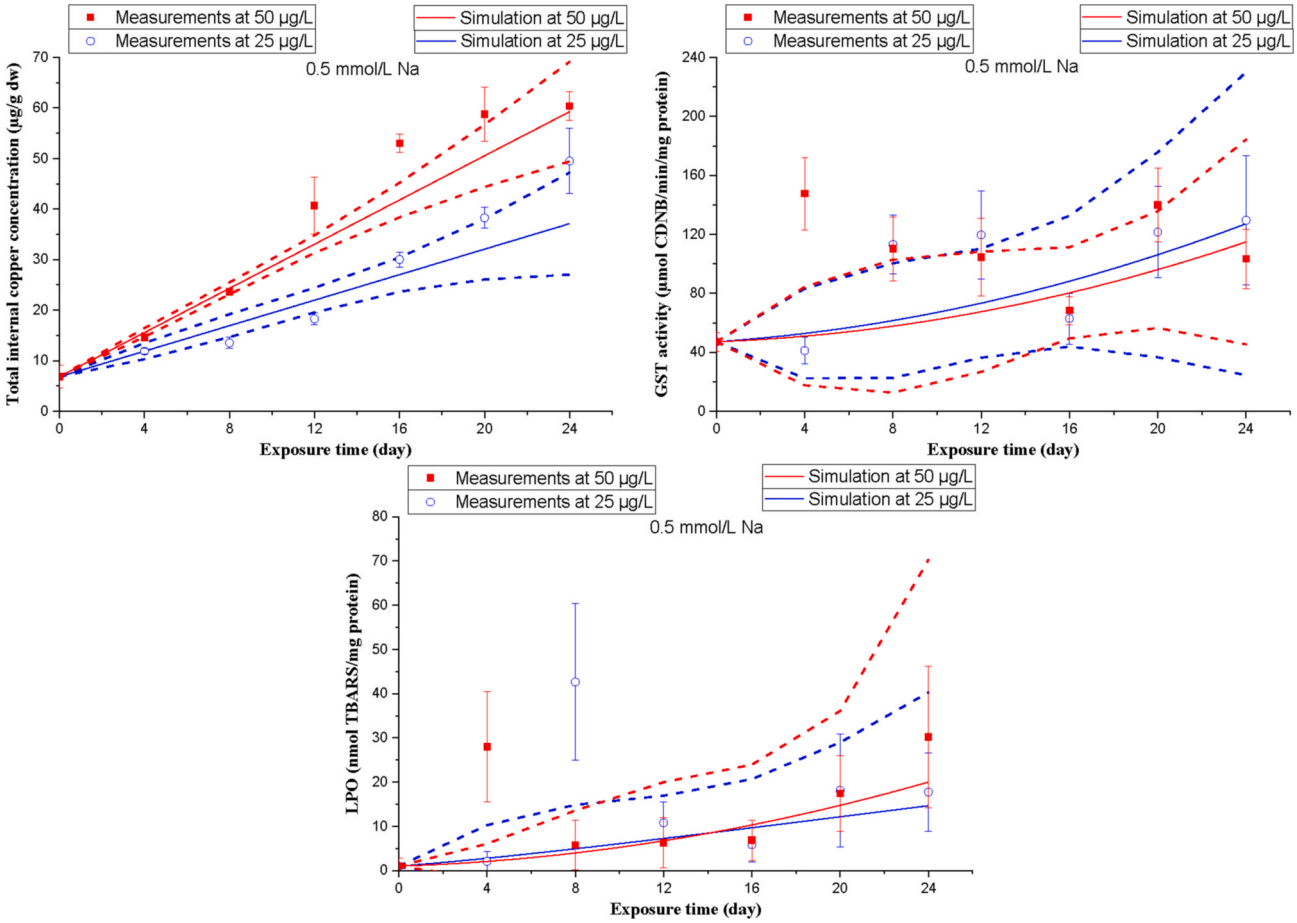

Fig. 2. Comparison between the modelled values and the measurements of total internal copper concentration, glutathione-S-transferase (GST) activity, and lipid peroxidation (LPO) in the zebra mussel exposed to Cu at nominal concentrations of 25 (blue signs) and 50 (red signs) μg/L for 24 days and 0.5 mmol/L Na^+. The transparent areas covered by the dashed lines and the solid lines represent the confidence interval and the mean of the estimations, respectively. The dots and bars represent the measurements (average and standard deviation, respectively). Data for other Na^+ concentrations is given in Fig. S3, Supporting Information. (For interpretation of the references to colour in this figure legend, the reader is referred to the Web version of this article.)

mmol/L (Table 3). Copper elimination was negligible at 25 μg/L, and more remarked at 50 μg/L (Table 3). Only at a Cu exposure concentration of 50 μg/L and a Na^+ concentration of 4.0 mmol/L, Cu was significantly eliminated, as demonstrated by the significant deviation of the elimination rate constant from zero (Table 3). Contrasting with such significant influence of the Cu exposure level, the Na^+ concentration in water did not affect the Cu uptake as shown by an overlap of the confidence intervals of the estimated uptake rates (mean ± error bound) at varied Na^+ concentrations in water (Table 3).

In addition, the simulation generated a non-significant difference in LPO level and GST activity with varied Cu exposure levels (Fig. 2; Fig. S4, Supporting Information), consistent with the observations (Figs. S2-S3, Supporting Information). Defining a significant difference between two measurements by an absence of an overlap of their ranges (average ± standard deviation), no solid pattern was revealed on the influence of Cu or Na on GST activity (Figs. S2-S3; Table S10, Supporting Information). Exposure to Cu at concentrations of 25 and 50 μg/L did not significantly affect LPO. During the 24-day exposure to dissolved Cu, LPO and GST activity in the zebra mussel fluctuated (Figs. S2-S3, Supporting Information). The alternation of decreases and increases in GST activity as well as LPO level during the exposure experiment was indicative of certain recovery of the antioxidant system (Figs. S2-S3, Supporting Information). The measurements of total internal Cu concentration, LPO level, and GST activity were generally within the

estimation, although the model could not explain the fluctuations of LPO and GST activity (Fig. 2; Fig. S6, Supporting Information). Active bounds in estimating the relationship between the simulated concentration of unbound Cu and responses of organisms (Table 3) indicated high uncertainty in the TD section.

4. Discussion

The instant and rapid reduction in Na accumulation as well as NKA activity is in agreement with the recognition of inhibited Na^+ influx and declined NKA activity as a main mechanism of acute Cu toxicity as simulated in Veltman et al. (2014). Model simulation displayed Cu-induced decreases in Na^+ uptake, consistent with empirical studies (Giacomin et al., 2013; Jorge et al., 2013). Together with these results, our findings that the Na^+ concentration had no significant effects on Cu uptake support the assumption of non-competitive inhibition of Cu^{2+} on NKA activity and Na^+ uptake. Compared to the biomarker responses, the current version of the TK-TD model simulates uptake kinetics of Cu better. Copper concentrations in the zebra mussel in the present study are comparable to those at similar exposure levels (Mersch and Pihan, 1993; Mersch et al., 1993), and slightly higher than the range in slightly or unpolluted water bodies (De Lafontaine et al., 2000; Faria et al., 2010; Alcaraz et al., 2011).

Similarly, both LPO level and GST activity recorded in the present study are in the range reported by others at sublethal concentrations (Jorge et al., 2013; Boukadida et al., 2017). A lack of significant effects of Cu at sublethal concentrations on LPO and GST activity is also consistent with conclusions from previous investigations (Table S10, Supporting Information). At environmentally relevant concentrations, Cu did not affect the antioxidant system of *Chlamys farreri*, as demonstrated by non-significant changes in GST activity (Zhang et al., 2010). De Lafontaine et al. (2000) presented limited variations of LPO in zebra mussels sampled from various sites in the St Lawrence River. Results of model calibration for *L. siliquoidea* and *D. polymorpha* indicated the responses of their antioxidant defence system against Cu toxicity. The difference in the patterns of LPO level and GST activity might be indicative of the capacity to respond to oxidative stress. For example, Maria and Bebianno (2011) concluded that Cu exposure did not influence GST activity in gills and the digestive gland of the mussel *Mytilus galloprovincialis*, but enhanced LPO in gills. These results imply an insufficient capacity of the mussel to modulate ROS formation. Non-significant differences in GST activity and LPO level between different exposure levels as well as the inability of the developed TK-TD model to capture the fluctuations in these biomarkers raise questions on the suitability of these biomarkers to represent chronic toxicity. According to Jorge et al. (2013), biomarkers evaluated on the whole-body soft tissue might not be suitable tools for monitoring responses of mussels chronically exposed to Cu. Therefore, the assessment should be extended to a variety of biomarkers to obtain a better understanding of mechanisms of chronic toxicity.

The limited capacity of the TK-TD model for explaining the variations in the biomarker responses might be attributed to the influence of environmental factors on the expression of oxidative stress-related biomarkers as well as the variations among tissues (Monserrat et al., 2007). The influence of Cu on glutathione metabolism depends on ambient concentration, exposure duration, and physiological and biochemical properties (Canesi et al., 1999). According to Gonzalez-Fernandez et al. (2015), LPO was positively related to nutritional status, and therefore to metabolic costs. Jorge et al. (2013) suggested that laboratory and test conditions, rather than the Cu exposure, accounted for the upgradation in ROS production over time. This suggestion was supported by increases in LPO and GST activity in unexposed mussels over time observed in the present study (Figs. S2-S3). Giacomin et al. (2013) suggested that freshwater mussels develope several mechanisms that contribute to their defence against ROS production. The potential influence of these counfounding factors should be considered to improve the performace of the model.

Chronic Cu toxicity was found not to be directly related to Cu bioaccumulation (Jorge et al., 2013). In long-term exposure at low concentrations, metals are mainly accumulated in low metabolically active fractions (Borgman et al., 1993). These results emphasise the necessity for further characterisation of TD, as further emphasised by higher uncertainty in TD than in TK in our TK-TD model. With the fact that the concentration of toxicants at sites of toxic actions is usually technically unmeasurable, TK-TD models are an effective method to mechanistically link responses of organisms to metal accumulation. The model calibration clearly unravelled mechanisms by which Cu inhibits NKA activity, i.e. by affecting the turnover rate as well as reducing the number of functional NKA. The model showed potential to extrapolate effects at the individual level to the molecular level whilst measurements at the molecular level would reduce uncertainty. The model provided another example for integrating BLM to TK-TD models, which had been implemented by Liang et al. (2021) for acute metal toxicity. The use of the affinity constants derived in the BLM facilitates model extrapolation to other species and other metals.

In the current version, some limitations might affect its potential for application and extrapolation. Influence of salinity on the abundance and molecular activity of NKA was excluded, following the negligible effects of salinity at the levels below 5 ppt reported by Sainting (1979). A consideration of salinity might improve the potential applicability of the model to various environmental conditions. Another limitation is related to the ODE describing the relationship between the simulated concentration of toxicologically available metals (i.e unbound to NKA) and responses of organisms. The ODE that covers damage accrual and recovery could not capture the fluctuations of LPO and GST activity. Consideration of adaptive or compensatory mechanisms might improve the relationship between the biological responses and the simulated concentration of metals at sites of toxic action or estimates of metal-toxicological availability. In addition, further validation with data sets covering NKA activity and a wider variety of oxidative-stress biomarkers will reduce uncertainty in model application.

5. Conclusions

A TK-TD model that includes different mechanisms of toxicity for evaluating biomarker responses at sublethal levels was developed for the first time and calibrated for freshwater mussels. An integration of affinity constants in the BLM to describe the binding of metals to enzymes into TK-TD models allows for simulating metal accumulation at sites of toxic action. NKA activity was related to the binding of Cu to NKA whilst LPO and GST activity were linked to the concentration of unbound Cu.

Author contributions

T.T. Yen Le: Conceptualisation, Methodology, Investigation, Validation, Visualization, Writing, Funding acquisition, Milen Nachev: Methodology, Investigation, Reviewing and Editing, Daniel Grabner: Methodology, Investigation, Reviewing and Editing, Miriam R. Garcia: Methodology, Reviewing and Editing, Eva Balsa-Canto: Methodology, Reviewing and Editing, A. Jan Hendriks: Validation, Reviewing and Editing, Willie J.G.M. Peijnenburg: Reviewing and Editing, Bernd Sures: Project administration, Validation, Reviewing and Editing.

Declaration of competing interest

The authors declare that they have no known competing financial interests or personal relationships that could have appeared to influence the work reported in this paper.

Acknowledgements

This research was financed by the Deutsche Forschungsgemeinschaft (DFG), Germany (LE 3716/2-1).

Appendix A. Supplementary data

Supplementary data to this article can be found online at https://doi.org/10.1016/j.envpol.2021.117645.

References

Alcaraz, C., Caiola, N., Ibanez, C., 2011. Bioaccumulation of pollutants in the zebra mussel from hazardous industrial waste and evaluation of spatial distribution using GAMs. Sci. Total Environ. 409, 898–904.

Arredondo, M., Nunez, M.T., 2005. Iron and copper metabolism. Mol. Aspect. Med. 26, 313–327.

Ashauer, R., Hintermeister, A., Caravatti, I., Kretschamann, A., Escher, B.I., 2010. Toxicokinetic and toxicodynamic modeling explains carry-over toxicity from exposure to diazinon by slow organism recovery. Environ. Sci. Technol. 44, 3963–3971.

Ashauer, R., Thorbek, P., Warinton, J., Wheeler, J., Maund, S., 2013. A method to predict and understand fish survival under dynamic chemical stress using standard ecotoxicity data. Environ. Toxicol. Chem. 32, 954–965.

Balsa-Canto, E., Alonso, A.A., Banga, J.R., 2010. An iterative identification procedure for dynamic modeling of biochemical networks. *BMC* Syst. Biol. 4, 11.

Boukadida, K., Cachot, J., Clerandeaux, C., Gourves, P.-Y., Banni, M., 2017. Early and efficient induction of antioxidant defense system in *Mytilus galloprovincialis* embryos exposed to metals and heat stress. Ecotoxicol. Environ. Saf. 138, 105–112.

Barata, C., Lekumberri, I., Vila-Escale, M., Prat, N., Porte, C., 2005. Trace metal concentration, antioxidant enzyme activities and suceptibility to oxidative stress in the tricoptera larvae *Hydropsyche exocellata* from the Llobregat river basin (NE Spain). Aquat. Toxicol. 74, 3–19.

Borgmann, U., Norwood, W.P., Clarke, C., 1993. Accumulation, regulation and toxicity of copper, zinc, lead and mercury in *Hyalella azteca*. Hydrobiologia 259, 79–89.

Bouskill, N.J., Handy, R.D., Ford, T.E., Galloway, T.S., 2006. Differentiating copper and arsenic toxicity using biochemical biomarkers in *Asellus aquaticus* and *Dreissena polymorpha*. Ecotoxicol. Environ. Saf. 65, 342–349.

Buege, J.A., Aust, S.D., 1978. Microsomal lipid peroxidation. Methods Enzymol. 52, 302–310.

Buffle, J., 1988. Complexation Reactions in Aquatic Systems: an Analytical Approach. Ellis Horwood, Chichester.

Bury, N.R., McGeer, J.C., Wood, C.M., 1999. Effects of altering freshwater chemistry on physiological responses of rainbow trout to silver exposure. Environ. Toxicol. Chem. 18, 49–55.

Canesi, L., Viarengo, A., Leonzio, C., Fillippelli, M., Gallo, G., 1999. Heavy metals and glutathione metabolism in mussel tissues. Aquat. Toxicol. 47, 67–76.

Cappello, T., Maisano, M., Giannetto, A., Parrino, V., Mauceri, A., Gasulo, S., 2015. Neurotoxicological effects on marine mussel *Mytilus galloprovincialis* caged at petrochemical contaminated areas (eastern Sicily, Italy): ^{1}H NMR and immunohistochemical assays. Comp. Biochem. Physiol., C 169, 7–15.

Caricato, R., Giordano, M.E., Maisano, M., Mauceri, A., Giannetto, A., Cappello, T., Parrino, V., Ancora Caliani, I., Bianchi, N., Leonzio, C., Mancini, G., Cappello Fasulo, S., Lionetto, M.G., 2019. Carbonic anhydrase integrated into a multimarker approach for the detection of the stress status induced by pollution exposure in *Mytilus galloprovincialis*: a field case study. Sci. Total Environ. 690, 140–150.

Chis, O., Banga, J.R., Balsa-Canto, E., 2011. GenSSI: a software toolbox for structural identifiability analysis of biological models. Bioinformatics 27, 2610–2611.

Coppola, F., Tavares, D.S., Henriques, B., Monteiro, R., Trindade, T., Soares, A.M.W.M., Figueira, E., Polese, G., Preira, E., Freitas, R., 2019. Remediation of arsenic from contaminated seawater using manganese spinel ferrite nanoparticles: ecotoxicological evaluation in *Mytillus galloprovincialis*. Environ. Res. 175, 200–212.

De Lafontaine, Y., Gagne, F., Blaise, C., Costan, G., Gagno, P., Chan, H.M., 2000. Biomarkers in zebra mussels (*Dreissena polymorpha*) for the assessment and monitoring of water quality of the St Lawrence River (Canada). Aquat. Toxicol. 50, 51–71.

Dietz, T.H., Lessard, D., Silverman, H., Lynn, J.W., 1994. Osmoregulation in *Dreissena polymorpha*: the importance of Na, Cl, K, and particularly Mg. Biol. Bull. 187, 76–83.

Else, P., Windmill, D.J., Markus, V., 1996. Molecular activity of sodium pumps in endotherms and ectotherms. Am. J. Physiol. 271, R1287–R1294.

Epstein, P.S., McIlwain, M., 1966. Actions of cupric salts on isolated cerebral tissues. Proc. R. Soc. Lond. Ser. B 166, 295.

Fan, W., Peng, R., Li, X., Ren, J., Liu, T., Wang, X., 2016. Effect of titanium dioxide nanoparticles on copper toxicity to *Daphnia magna* in water: role of organic matter. Water Res. 105, 129–137.

Faria, M., Huertas, D., Soto, D.X., Grimalt, J.O., Catalan, J., Riva, M.C., Barata, C., 2010. Contaminant accumulation and multi-biomarker responses in field collected zebra mussels (*Dreissena polymorpha*) and crayfish (*Procambarus clarkii*), to evaluate toxicological effects of industrial hazardous dumps in the Ebro river (NE Spain). Chemosphere 78, 232–240.

Garcon, D.P., Masui, D.C., Mantelatto, F.L.M., Furriel, R.P.M., McNamara, J.C., Leone, F. A., 2009. Hemolymph ionic regulation and adjustments in gill (Na^+, K^+)-ATPase activity during salinity acclimation in the swimming crab *Callinectes ornatus* (Decapoda, Brachyura). Comp. Biochem. Physiol. A 154, 44–55.

Giacomin, M., Gillis, P.L., Bianchini, A., Wood, C.M., 2013. Interactive effects of copper and dissolved organic matter on sodium uptake, copper bioaccumulation, and oxidative stress in juvenile freshwater mussels (*Lampsilis siliquoidea*). Aquat. Toxicol. 144–145, 105–115.

Gomes, T., Pinheiro, J.P., Cancio, I., Pereira, C.G., Cardoso, C., Bebianno, M.J., 2011. Effects of copper nanoparticles exposure in the mussel *Mytilus galloprovincialis*. Environ. Sci. Technol. 45, 9356–9362.

Gonzalez-Fernandez, C., Albentosa, M., Campillo, J.A., Vinas, L., Fumega, J., Franco, A., Besada, V., Gonzalez-Quijano, A., Bellas, J., 2015. Influence of mussel biological variability on pollution biomarkers. Environ. Res. 137, 14–31.

Goswami, P., Hariharan, G., Godhantaraman, N., Munuswamy, N., 2014. An integrated use of multiple biomarkers to investigate the individual and combined effect of copper and cadmium on the marine green mussel (*Perna viridis*). J. Environ. Sci. Health A 49, 1564–1577.

Grosell, M., Nielsen, C., Bianchini, A., 2002. Sodium turnover rate determines sensitivity to acute copper and silver exposure in freshwater animals. Comp. Biochem. Physiol., C 133, 287–303.

Habig, W.H., Pabst, M.J., Jakoby, W.B., 1974. Glutathione S-Transferases: the first enzymatic step in mercapturic acid formation. J. Biol. Chem. 249, 7130–7139.

Halliwell, B., Gutteridge, M.C., 1984. Oxygen toxicity, oxygen radicals, transition metals and disease. Biochem. J. 219, 1–14.

Jager, T., Albert, C., Preuss, T.G., Ashauer, R., 2011. General unified threshold model for survival – a toxicokinetic-toxicodynamic framework for ecotoxicology. Environ. Sci. Technol. 45, 2529–2540.

Jorge, M.B., Loro, V.L., Bianchini, A., Wood, C.M., Gillis, P.L., 2013. Mortality, bioaccumulation and physiological responses in juvenile freshwater mussels (*Lampsilis siliquoidea*) chronically exposed to copper. Aquat. Toxicol. 126, 137–147.

Jorge, M.B., Bianchini, A., Wood, C.M., Gillis, P.L., 2018. Copper uptake, patterns of bioaccumulation, and effects in glochidia (larvae) of the freshwater mussel (*Lampsilis cardium*). Environ. Toxicol. Chem. 37, 1092–1103.

Kone, B.C., Brenner, R.M., Gullams, S.R., 1990. Sulfhydryl-reactive heavy metals increase cell membrane K^+ and Ca^{2+} transport in renal proximal tubule. J. Membr. Biol. 113, 1–12.

Krstic, D., Krinulovic, K., Vasic, V., 2005. Inhibition of Na^+,K^+-ATPase by metal ions and prevention and recovery of inhibited activities by chelators. J. Enzym. Inhib. Med. Chem. 20, 469–476.

Kulac, B., Atli, G., Canli, M., 2013. Response of ATPases in the osmoregulatory tissues of freshwater fish *Oreochromis niloticus* exposed to copper in increased salinity. Fish Physiol. Biochem. 39, 391–401.

Le, T.T.Y., Garcia, M.R., Nachev, M., Grabner, D., Balsa-Conto, E., Hendriks, A.J., Sures, B., 2018. Development of a PBPK model for silver accumulation in chub infected with acanthocephalan parasites. Environ. Sci. Technol. 52, 12514–12525.

Le, T.T.Y., Garcia, M.R., Grabner, D., Nachev, M., Balsa-Canto, E., Hendriks, J., Zimmermann, S., Sures, B., 2020. Mechanistic simulation of bioconcentration kinetics of waterborne Cd, Ag, Pd, and Pt in the zebra mussel *Dreissena polymorpha*. Chemosphere 242, 124967.

Le, T.T.Y., Grabner, D., Nachev, M., Peijnenburg, W.J.G.M., Hendriks, A.J., Sures, B., 2021. Modelling copper toxicokinetics in the zebra mussel, *Dreissena polymorpha*, under chronic exposures at variou pH and sodium concentrations. Chemosphere 267, 129278.

Lee, T.-H., Feng, S.-H., Lin, C.-H., Hwang, Y.-H., Huang, C.-L., Hwang, P.-P., 2003. Ambient salinity modulates the expression of sodium pumps in branchial mitochondria-rich cells of Mozambique Tilapia, *Oreochromis mossambicus*. Zool. Sci. 20, 29–36.

Li, J., Lock, R.A.C., Klaren, P.H.M., Swarts, H.G.P., Schuurmans Stekhoven, F.M.A.H., Wendelaar Bonga, S.E., Flik, G., 1996. Kinetics of Cu^{2+} inhibition of Na^+/K^+-ATPase. Toxicol. Lett. 87, 31–38.

Liang, W.-Q., Xie, M., Tan, Q.-G., 2021. Making the Biotic Ligand Model kinetic, easier to develop, and more flexible for deriving water quality criteria. Water Res. 188, 116548.

Ligon, T.S., Fröhlich, F., Chiş, O.T., Banga, J.R., Balsa-Canto, E., Hasenauer, J., 2018. GenSSI 2.0: multi-experiment structural identifiability analysis of SBML models. Bioinformatics 34, 1421–1423. https://doi.org/10.1093/bioinformatics/btx735.

Lowry, O.H., Rosebrough, N.J., Farr, A.L., Randall, R.J., 1951. Protein measurement with the folin phenol reagent. J. Biol. Chem. 193, 265–275.

Maellaro, E., Casini, A.F., Del-Bello, B., Comporti, M., 1990. Lipid peroxidation and antioxidant systems in the liver injury produced by glutathione depleting agents. Biochem. Pharmacol. 39, 1513–1521.

Maria, V.L., Bebianno, M.J., 2011. Antioxidant and lipid peroxidation responses in *Mytilus galloprovincialis* exposed to mixture of benzo(a)pyrene and copper. Comp. Biochem. Physiol., C 154, 56–63.

McGeer, J.C., Playle, R.C., Wood, C.M., Galvez, F., 2000. A physiological based biotic ligand model for predicting the acute toxicity of waterborne silver to rainbow trout in freshwaters. Environ. Sci. Technol. 34, 4199–4207.

Mersch, J., Pihan, J.-C., 1993. Simultaneous assessment of environmental impact on condition and trace metal availability in zebra mussels *Dreissena polymorpha* transplanted into the Wiltz River, Luxembourg. Comparison with the aquatic moss. Arch. Environ. Contam. Toxicol. 25, 353–364.

Mersch, J., Morhain, E., Mouvet, C., 1993. Laboratory accumulation and depuration of copper and cadmium in the freshwater mussel *Dreissena polymorpha* and the aquatic moss *Rhynchostegium riparioides*. Chemosphere 27, 1475–1485.

Morgan, I.J., Henry, R.P., Wood, C.M., 1997. The mechanism of acute silver nitrate toxicity in freshwater rainbow trout (*Oncorhynchus mykiss*) in inhibition of gill Na^+ and Cl^- transport. Aquat. Toxicol. 38, 145–163.

Monserrat, J.M., Martinez, P.E., Geracitano, L.A., Amado, L.L., Martins, C.M.G., Pinho, G. L.L., Chaves, I.S., Ferreira-Cravo, M., Ventura-Lima, J., Bianchini, A., 2007. Pollution biomarkers in estuarine animals: critical review and new perspectives. Comp. Biochem. Physiol., C 146, 221–234.

Nishikawa, T., Lee, I.S.M., Shiraishi, N., Ishikawa, T., Ohta, Y., Nishikimi, M., 1997. Identification of S100b protein as copper-binding protein and its suppression of copper-induced cell damage. J. Biol. Chem. 272, 23037–23041.

Ohkawa, H., Ohishi, N., Yagi, K., 1979. Assay for lipid peroxides in animal tissues by thiobarbituric acid reaction. Anal. Biochem. 95, 351–358.

Osterauer, R., Marschner, L., Betz, O., Gerberding, M., Sawasdee, B., Cloetens, P., Haus, N., Sures, B., Triebskorn, R., Koehler, H.-R., 2010. Turning snails into slugs: induced body plan changes and formation of an internal shell. Evol. Dev. 12, 475–483.

Paquin, P.R., Di Toro, D.M., Santore, R.C., Trivedi, D., Wu, K.B., 1999. A Biotic Ligand Model of the Acute Toxicity of Metals. III. Application to Fish and Daphnia Exposure to Silver, Section 3 in Integrated Approach to Assessing the Bioavailability and Toxicity of Metals in Surface Waters and Sediments, a Submission to the EPA Science Advisory Board. Office of Water, Office of Research and Development, Washington, DC, pp. 3–59.

Petala, M., Kokokiris, L., Samaras, P., Papadopoulos, A., Zouboulis, A., 2009. Toxicological and ectotoxic impact of secondary and tertiary treated sewage effluents. Water Res. 43, 5063–5074.

Piermarini, P.M., Evans, D.H., 2000. Effects of environmental salinity of Na^+/K^+-ATPase in the gills and rectal gland of a euryhaline elasmobranch (*Dasyatis sabina*). J. Exp. Biol. 203, 2957–2966.

Poli, G., Chiarpotto, E., Albano, E., Biasi, F., Ceccini, G., Dianzani, M.U., 1986. Iron overload: experimental approach using rat hepatocytes in single cell suspensions. In: Dianzani, M.U., Gentillini, P. (Eds.), Chronic Liver Disease, Frontiers in Gastrointestinal Research, pp. 38–49.

Reed, J.D., 1990. Glutathione: toxicological implications. Annu. Rev. Pharmacol. Toxicol. 30, 603–631.

Rikans, L.E., Hornbrook, K.R., 1997. Lipid peroxidation, antioxidant protection and aging. Biochim. Biophys. Acta 1361, 116–127.

Sainting, D.G., 1979. The Role of $Na^+ + K^+$-activated Adenosine Triphosphatase in the Osmoregulating Marsh Clam, *Rangia Cuneata*. University of Richmond.

Towle, D.W., 1984. Membrane-bound TAPases in arthropod ion-transporting tissues. Am. Zool. 24, 177–185.

Turner, N., Else, P.L., Hulbert, A.J., 2005. An allometric comparison of microsomal membrane lipid composition and sodium pump molecular activity in the brain of mammals and birds. J. Exp. Biol. 208, 371–381.

Vasic, V., Jovanovic, D., Krstic, D., Nikezic, G., Horvat, A., Vujisic, L., Nedejkovic, N., 1999. Prevention and recovery of $CuSO_4$-induced inhibition of Na^+/K^+-ATPase and Mg^{2+}-ATPase in rat brain synaptosomes by EDTA. Toxicol. Lett. 110, 95–104.

Vasic, V.M., Colovic, M.B., Krstic, D.Z., 2009. Mechanism of Na^+/K^+-ATPase and Mg^{2+}-ATPase inhibition by metal ions and complexes. Hem. Ind. 63, 499–509.

Veltman, K., Hendriks, A.J., Huijbregts, M.A.J., Wannaz, C., Jolliet, O., 2014. Toxicokinetic toxicodynamic modeling of Ag toxicity in freshwater organisms: whole-body sodium loss predicts acute mortality across aquatic species. Environ. Sci. Technol. 48, 14481–14489.

Vijayavel, K., Anbuselvam, C., Balasubramanian, M.P., 2007. Antioxidant effect of the marine algae *Chlorealla vulgaris* against naphthalene-induced oxidative stress in the albino rats. Mol. Cell. Biochem. 303, 39–44.

Wang, C.M., Al-Reasi, H.A., Smith, D.S., 2011. The two faces of DOC. Aquat. Toxicol. 105, 3–8.

Waykar, B., Lomte, V.S., 2001. Total protein alteration in different tissues of freshwater bivalve, *Parisians cylindrica* after cypermethrin exposure. Ecol. Environ. Conserv. 7, 465–469.

Zhang, Y., Song, J., Yuan, H., Xu, Y., He, Z., Duan, L., 2010. Biomarker responses in the bivalve (*Chlamys farreri*) to exposure of the environmentally relevant concentrations of lead, mercury, copper. Environ. Toxicol. Pharmacol. 30, 19–25.